

Hot electron of steady-state transport in submicrometer ZnSe and ZnS n⁺-i(n)-n⁺ diodes

H. Arabshahi¹, M. Rezaee Rokn-Abadi¹, F. Badiieyan¹ and M.R. Khalvati²

¹Physics Department, Ferdowsi University of Mashhad, Mashhad, Iran

²Physics Department, Shahrood University of Technology, Shahrood, Iran

arabshahi@um.ac.ir

Abstract

Monte Carlo simulation of steady-state electron transport in ZnSe and ZnS diodes of n⁺-i(n)-n⁺ structure with a 0.2 μm active layer length is described. The anode voltage ranges from 1 to 5 V. The distributions of electron energies and electron velocities, and the profiles of the electron density, electric field, potential and average electron velocity are computed. Based on these data, the near ballistic nature of the electron transport in the 0.2 μm long diode and the importance of the back-scattering of electrons from the anode n⁺-layer are discussed. Also, the effects of the lattice temperature and doping on the length of the active layer are discussed. Our calculations show that electron reach to a higher drift velocity in the ZnSe than ZnS. So ZnSe material is a good candidate for high power device fabrication.

Keywords: Active layer, diode, drift velocity, ballistic.

Introduction

Wide band gap ZnSe and ZnS have two main uses in commercial devices, providing bright LEDs emitting diodes and high power and high temperature heterojunction field effect transistors (HFETs) which can sustain high current densities at elevated temperatures (Arabshahi *et al.*, 2008). It has been shown that ZnSe and ZnS have large peak electron velocity and can be an important candidate for high frequency application. A wide energy band gap leads to a low intrinsic carrier concentration, which enables a more precise control of free carrier concentration over a wide range of temperatures, and hence the devices made of this kind of material will be operable at high temperatures with large breakdown voltage (Fischetti & Laux, 1991).

Recently, there has been considerable interest in the electron transport in submicron ZnSe and ZnS devices for possible high-frequency and high-speed applications. As the transit time of electrons in a device becomes comparable, or less than, the mean free time between collisions, the electrons will move more or less ballistically in the device, and will obtain very high velocities. Simulations of these phenomena in a diode structure have so far only been carried out for a very small anode voltage, or with rather artificial cathode and anode structures (Izuka & Fukuma, 1990). However, simulations for higher anode voltages are needed in view of the situation in practical devices where engineering problems call for anode voltages of no less than about the Schottky barrier height or the p-n junction barrier height (Besikci *et al.*, 2000). The boundary conditions are important as they have significant influence on the space-charge-limited current flow which becomes dominant in submicron devices (Bhuiyam *et al.*, 2003). In this paper we report an ensemble Monte Carlo simulation of the electron transport in a submicron ZnSe and ZnS diodes with highly doped n⁺-layer employed as cathode and anode. The

anode voltage applied to the diode ranges from 1 to 5 V. This article is organized as follows. Details of the device fabrication and Monte Carlo model which is used in the simulated device are presented below and the results for simulations carried out on the device follow thereafter.

Simulation models

An ensemble Monte Carlo simulation have been carried out to simulate the electron transport properties in ZnSe and ZnS based n⁺-i(n)-n⁺ diodes. The method simulates the motion of charge carriers through the device by following the progress of 10⁴ superparticles. These particles are propagated classically between collisions according to their velocity, effective mass and the prevailing field (Besikci *et al.*, 2000). The selection of the propagation time, scattering mechanism and other related quantities is achieved by generating random numbers and using this numbers to select, for example, a scattering mechanism. Our self-consistent Monte Carlo simulation was performed using an analytical band structure model consisting of five non-parabolic ellipsoidal valleys (Foutz *et al.*, 1997). The scattering mechanisms considered in the model are acoustic, polar optical, ionized impurity, piezoelectric and nonequivalent intervalley scattering. The nonequivalent intervalley scattering is between Γ, U and K valleys. For this work the Γ valley, the two equivalent K valleys, and the six equivalent U valleys were represented by spherical, nonparabolic, analytical effective mass expressions of the following form (Kane, 1957; Jacoboni & Reggiani, 1983)

$$\varepsilon(1 + \alpha\varepsilon) = \frac{\hbar^2 k^2}{2m^*} \quad (1)$$

The low energy effective masses, m^{*}, and the nonparabolicity factors, α, were obtained by matching equation 1 to the first principles bands (Arabshahi *et al.*, 2008).

Acoustic and piezoelectric scattering are assumed elastic and the absorption and emission rates are combined under the equipartition approximation, which is valid for lattice temperatures above 77 K. Elastic ionized impurity scattering is described using the screened Coulomb potential of the Brooks-Herring model (Bhuiyam *et al.*, 2003).

Steady-state results of high field transport studies have been obtained for lattice temperatures up to 600 K, in order to gain some insight into the hot carrier transport and the energy distribution function that would be generated in the gate-drain region of a power field effect transistor (Vurgaftman & Meyer, 2001). The material and valley parameters necessary for calculating the scattering probabilities used in the present Monte Carlo simulation are listed in Table 1. The $n^+ - i(n) - n^+$ diode structure has an active n^+ -layers with a $0.2 \mu\text{m}$ length which is sandwiched between a $0.2 \mu\text{m}$ cathode and anode n^+ -layers that are abruptly are doped to $2 \times 10^{17} \text{cm}^{-3}$.

Results and Discussion

Fig.1 shows the simulated velocity-field characteristics of wurtzite ZnSe and ZnS semiconductors at 300 K, with a background doping concentration of 10^{17}cm^{-3} , and with the electric field applied along c -axes. The simulations suggest that the peak drift velocity for ZnSe is as high as $3 \times 10^5 \text{ms}^{-1}$, while that for ZnS is about $\sim 1.2 \times 10^5 \text{ms}^{-1}$. At higher electric fields, intervalley optical phonon emission dominates, causing the drift velocity to saturate at around $1 \times 10^5 \text{ms}^{-1}$ for ZnS.

Fig.2 show the free electron density as function of device length in bias of 1, 3 and 5 V for ZnSe and ZnS $n^+ - i(n) - n^+$ diodes. It is apparently from the figure that in absence of any external voltage, electrons diffuse from the n^+ -region into the channel. This diffusing of electrons is due to uniform doping profile along device length (Newman *et al.*, 1989). This causes a dipole of charge at the two surface of each homojunction which induces a field opposite to the diffusion of electrons from n^+ -region to the channel. When a voltage is applied to contacts, electrons are injected to the channel by anode and cathode; therefore the density of electron rises to its primitive value in this region. The electron density behavior in the channel leads to create a non-uniform potential profile and consequently electric field inside the channel which showed in Fig.3 and 4, respectively. As we expect from Fig.2, potential have slightly decrease at first homojunctions, then it increase steeply until reach to a value of applied voltage near the second homojunctions. Electric field inside the structure is obtained by calculation of distinguish of the potential inside the structure. Also with increasing the applied voltage, higher electric field can be created inside the channel. Since in this voltage range electric field of structure is little than threshold value in both of ZnSe and ZnS. Electric field in almost the entire channel region is an accelerating field that provides a favorable transport condition for electrons (Ridley,

1993). In this way, in the center of the $n^+ - i(n) - n^+$ structure, electron gain energy from the field.

In Fig.6 electron drift velocity as function of applied voltage was reported at different voltages in both ZnSe and ZnS $n^+ - i(n) - n^+$ diode. With increasing applied voltage, electron velocity increase inside the channel. The electrons mobility in ZnSe structure is $> \text{ZnS}$ in the same voltage. It is partly due to heavy effective electron mass in ZnSe in comparison to ZnS. Another effect is the larger electric field in the channel as it can be seen from Fig.5.

Conclusions

The results of simulations of electron transport in $n^+ - i(n) - n^+$ ZnSe and ZnS diodes have been reported. The diodes have highly doped n^+ -layers serving as the cathode and anode. The anode voltages ranged from 1 to 5 V at room lattice temperature. The electrons injected from the cathode initially travel quasi-ballistically but there is substantial transfer to the upper satellite valleys as the anode is approached, resulting in a reduced average electron velocity in that region. Due to higher velocity-field characteristic it is shown that ZnSe based devices should expect to have more performance than ZnS material.

Table 1. Material parameter selections for ZnSe & ZnS.

Parameters	ZnS	ZnSe
Density $\rho(\text{kgm}^{-3})$	4075	5420
Longitudinal sound velocity $v_s(\text{ms}^{-1})$	5868	4580
Low-frequency dielectric constant ϵ_0	9.6	9.2
High-frequency dielectric constant ϵ_∞	5.7	15
Acoustic deformation potential $D(\text{eV})$	4.9	4.5
Polar optical phonon energy (eV)	0.04	0.03
Intervalley deformation potentials (10^7eVm^{-1})	1	1
Electron effective mass (m^*)	0.28	0.17
Nonparabolicity (eV^{-1})	0.69	0.67

References

1. Arabshahi H, Khalvati MR and Rezaee Rohn-Abadi M (2008) Comparison of steady state and transient electron transport in InAs, InP and GaAs. *Modern Phys.Lett. B.* 22 (17), 1695-1702.
2. Arabshahi H, Khalvati MR and Rezaee Rohn-Abadi M (2008) Monte Carlo modeling of hot electron transport in bulk AlAs, AlGaAs and GaAs at room temperature. *Modern Phys. Lett. B.* 22 (18), 1777-1784.
3. Besikci B, Bakir M and Tanatar U (2000) Hot electron simulation devices. *J. Appl. Phys.* 88 (3), 1243-1247.
4. Bhapkar U V and Shur M S (1997) Ensemble Monte Carlo study of electron transport in wurtzite In. *J. Appl. Phys.* 82, 1649-1654.
5. Bhuiyam S, Senoh M and Mukai T (2003) Comparison of steady state and transient electron *Appl. Phys. Lett.* 62, 2390-2395.
6. Brennan K, Hess K, Tang JY and Iafrate GT (1983) High field electron transport properties. *IEEE Trans.Electron Devices*, 30, 1750-1755.

Fig. 1. Calculated steady-state electron drift velocity in bulk wurtzite ZnSe and ZnS using non-parabolic band models at room temperature

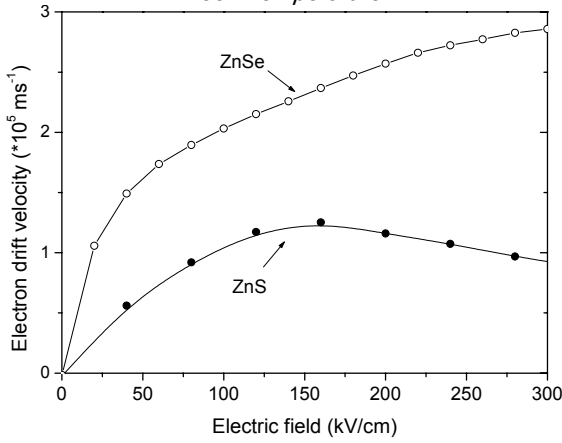


Fig. 2. Electron density along ZnSe and ZnS $n^+ - i(n) - n^+$ diode

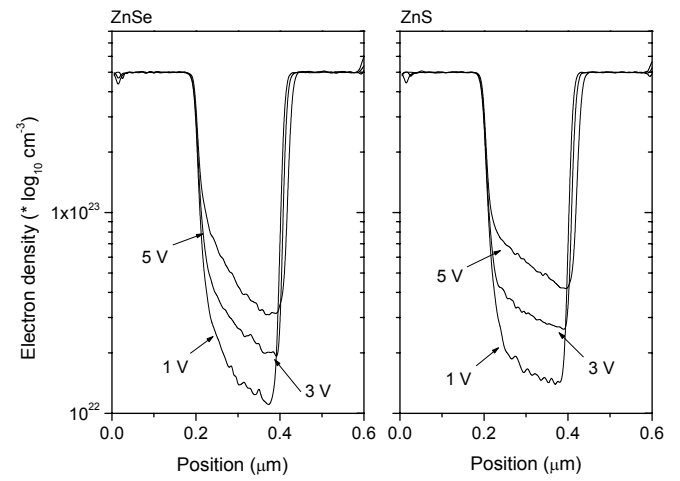


Fig. 3. Potential along ZnSe and ZnS $n^+ - i(n) - n^+$ diode

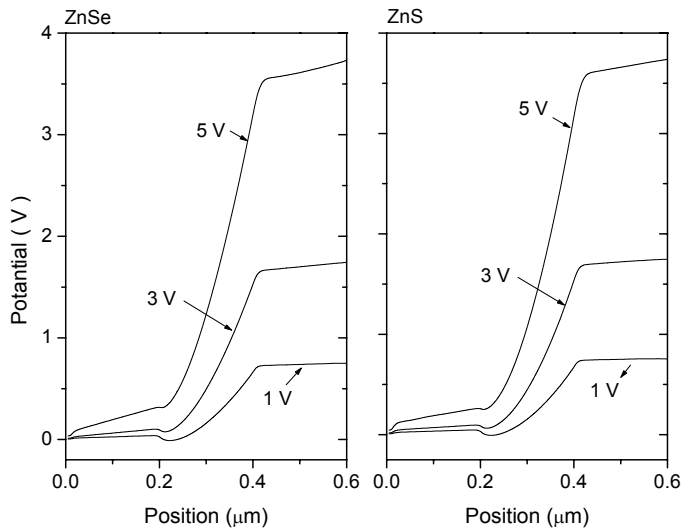


Fig. 4. Electric field along ZnSe and ZnS $n^+ - i(n) - n^+$ diode

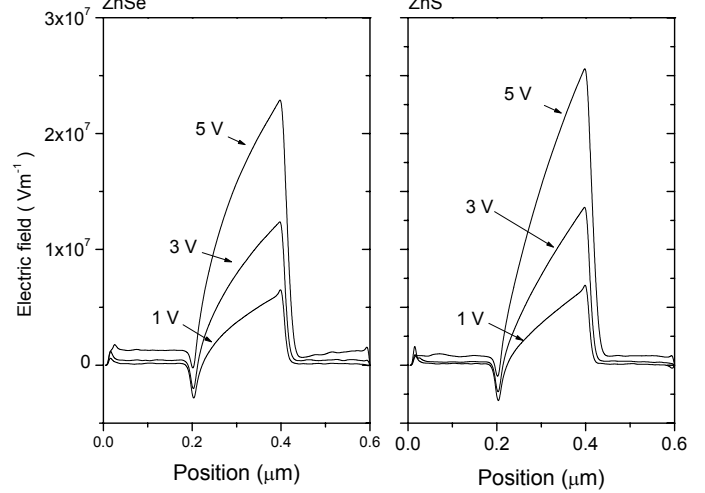


Fig. 5. Electric field along ZnSe and ZnS $n^+ - i(n) - n^+$ diode

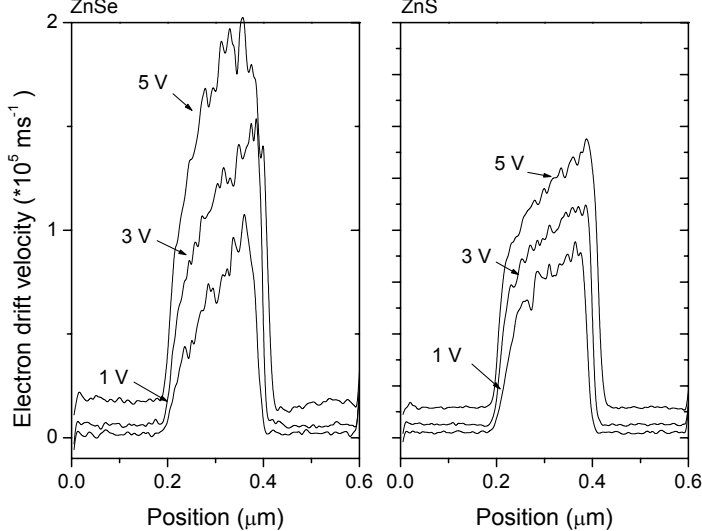
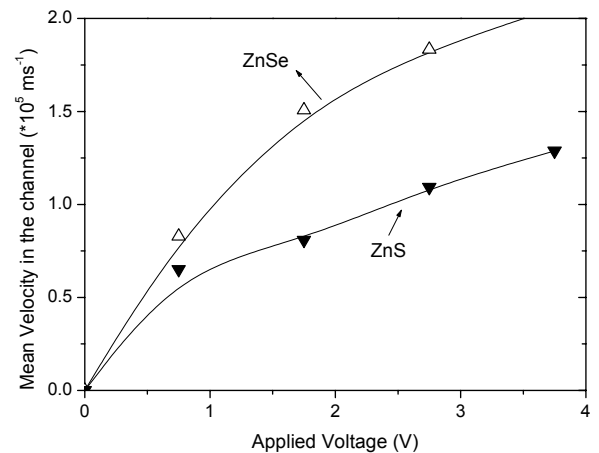


Fig. 6. Electron drift velocity as function of applied voltage through the simulated device





7. Fischetti MV and Laux SE (1991) Low field electron mobility in GaN. *IEEE Trans. Electron Devices*, 38, 650-655.
8. Foutz BE, Eastman LE, Bhapkar UV and Shur M (1997) Full band Monte Carlo simulation of Zincblende GaN MESFET's including realistic impact ionization rates. *Appl. Phys. Lett.* 70, 2849-2854.
9. Ghani B, Hashimoto A and Yamamoto A (2003) High temperature characteristics of AlGaIn/GaN modulation doped field-effect transistors. *J. Appl. Phys.* 94, 2779-2783.
10. Izuka J and Fukuma M (1990) Full-band polar optical phonon scattering analysis and negative differential conductivity in wurtzite GaN. *Solid-State Electron*, 3, 27-33.
11. Jacoboni J and Lugli P (1989) The Monte Carlo method for semiconductor and device simulation. Springer-Verlag.
12. Jacoboni J and Reggiani L (1983) The Monte Carlo simulation of Semiconductor and Devices. *Rev. Modern Phys.* 55 (3), 665-663.
13. Kane EO (1957) Band structure calculation in group III and IV materials. *J. Phys. Chem. Solids*, 1, 249-253.
14. Martienssen M and Warlimont H (2005) Springer hand book of condensed Matter and Materials Data, Springer.
15. Newman N, Schilfgaarde V, Kendelewicz T and Spicer WE (1989) GaN based transistor for high power applications. *Mater. Res. Soc. Symp. Proc.* 21, 54-59.
16. Ridley BK (1993) Quantum processes in semiconductors. Clarendon Press. Oxford.
17. Vurgaftman I and Meyer JI (2001) A review for GaN based devices. *J. Appl. Phys.* 89(11), 887-889.
18. Yu Y and Cardona M (2001) Fundamentals of Semiconductors. 3rd ed., Springer, Berlin, Heidelberg.